

Embedded Light Sensing In Mechanical Metamaterials

Johannes Kahlen*

s8jokahl@stud.uni-saarland.de

Saarland University, Saarland Informatics Campus
Saarbrücken, Germany

Rifat Rahman Turjo*

ritu00001@stud.uni-saarland.de

Saarland University, Saarland Informatics Campus
Saarbrücken, Germany

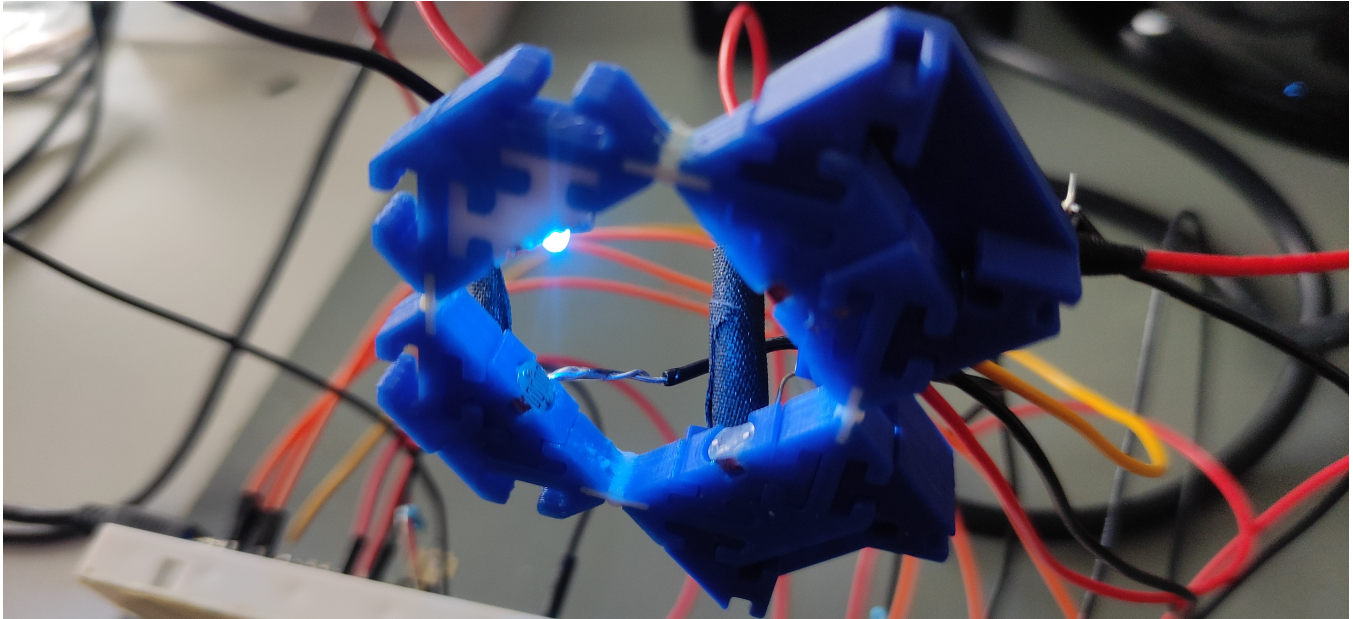


Figure 1: 3D fabricated metamaterial light sensor. A light-emitting diode (left) shines a blue light on one of the light-dependent resistors (right) embedded into the cell structure.

ABSTRACT

The recent development of 3D printing technologies led to the fabrication of unique structures with novel properties known as metamaterials. In recent years, there has been a push to design metamaterial devices with sensing capabilities with the aid of technologies such as capacitive-based sensing. In this paper, we propose a novel design for a metamaterial structure whose sensing capabilities are based on light-sensitive components. Figure 1 shows our 3D-printed metamaterial light sensor. The aim was to create a metamaterial device whose sensors are able to take in light as raw inputs, sense and process continuous deformation of the physical structure, and utilize sensor fusion principles to visually replicate the extent of deformation of the physical structure virtually in software. Through our work, we have been able to determine the capabilities of metamaterial light sensors as input devices in for applications in the field of Human-Computer Interaction.

1 INTRODUCTION

The driving force behind the study of metamaterials lies in the fact that engineers are now able to design and fabricate internal structures with unique properties that are absent in nature. Ion et al. in [4] describes metamaterials as structures that are able to cover large design spaces due to their thousands of degrees of freedom. It is the geometry of the structure that allows it to have unique properties such as volume change, shock absorption, localized elasticity, and much more. In addition to prior work on metamaterial design that was heavily focused on external design, researchers now have also emphasized the importance of internal design. In brief, by dividing the internal structure of these objects into repeating cellular grids and altering their parameters we can design metamaterials with numerous mechanical properties. This led to the rise of mechanical metamaterials and the possibility of developing input devices and tools in the field of HCI.

In the last decade, the advancement of metamaterials has developed significantly, deepening our understanding of the cell structures composition which are integral to their mechanisms [5]. This has led to the creation of unique metamaterial devices whose deformation can be interpreted as input signals that can be processed resulting in a desirable output quantity that can be measured. However, extensive research in the domain of metamaterial sensing is mostly geared toward the discrete domain. For instance, in their

*All authors contributed equally to this research.

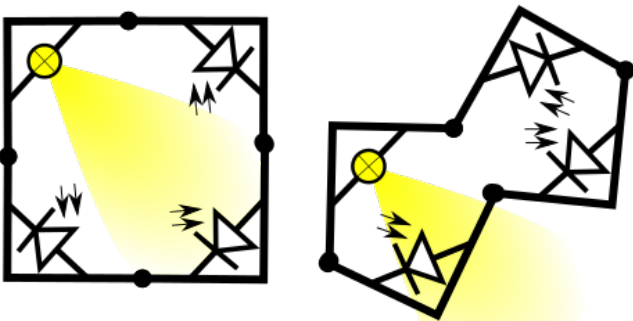


Figure 2: Initial concept of the metamaterial sensor. Left: Light from the LED is projected onto one of the light-dependent resistors. Right: Deformation of the sensor causes the LED to project more directed light on a particular light-dependent resistor.

individual works [3, 6] demonstrated means of embedding discrete signals and digital logic into mechanical metamaterials. Unfortunately, these devices are unable to perform the computation necessary for processing the continuous deformation of mechanical metamaterial structures. Furthermore, the majority of the prior research in the field revolves around embedding capacitive-based sensors into mechanical structures. In recent years, researchers have been focusing on the implementation of magnetic-based sensing techniques on metamaterial devices [1, 2, 8]. In contrast, our project delves into an untapped field for metamaterial sensing: the visible spectrum.

In this paper, a novel design of metamaterial sensors utilizing light-sensitive components has been presented to measure continuous deformation sensing of the mechanical structure and provide estimations of deformation parameters. We elaborate on the structure design of our deformable metamaterial sensor consisting of cell flexures and connecting components, enabling one to create and modify existing cells on the fly. We also detail the electronic circuit design embedded into the cell structure as well as the software implementation allowing us to calculate the approximation of the deformation occurring and visualize the output demonstrating the location and degree of deformation.

The design of the metamaterial light sensor is based on the design principles of deformable metamaterial structures presented in Ou. et al[7]. The cell structure consists of two repeating building blocks: the cell walls referred to as flexures and the connecting components where the electronic components are embedded. For the circuit design a surface-mounted light emitting diode (LED), as well as light-dependent resistors (LDR), are used as shown in Figure 2. Lastly, in software, a sensor fusion algorithm has been implemented whose inputs are the raw values from the light-dependent resistors and combines them to provide an estimation of the extent of deformation taking place at different points of the cell structure when the sensor is deformed.

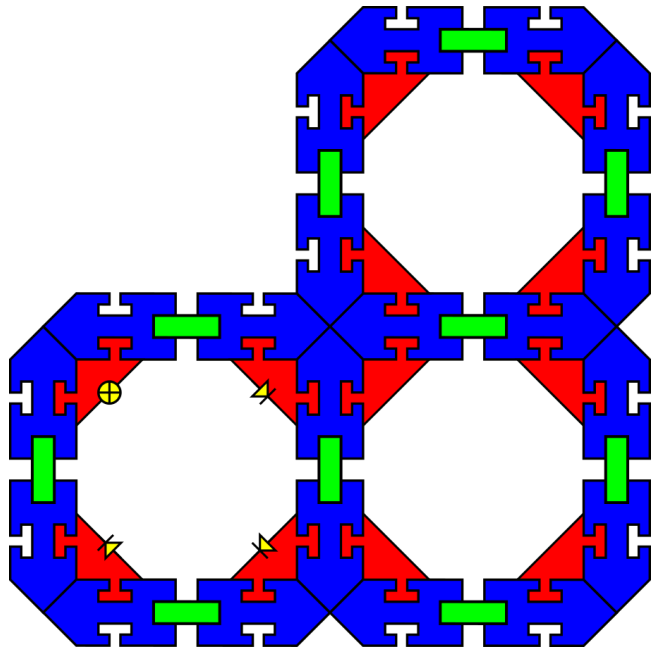


Figure 3: Metamaterial light sensor cell design. Blue: cell wall structure made of PLA, Green: Linkage structure made of TPU, Red: Edge component with slots and notches for circuit components for the sensor.

2 DESIGN AND IMPLEMENTATION

2.1 Cell Structure Design

In the initial design of the metamaterial sensor, we took inspiration from [7] and thus created cell components consisting of primary three parts as shown in Figure 3. Firstly we have the blue cell wall structures that were fabricated from a hard filament substance such as polylactic acid(PLA). Following that, there is the green linkage structure made from a flexible type of filament such as thermoplastic polyurethane(TPU) which connects the two halves of the cell wall creating the cell flexures. Finally, two flexures are then connected together by the red edge components, which are also made of PLA. The modular design allows for components to snap fit into places in a Lego block-like fashion creating a single sensor cell. This can then be repeated to create a grid of cell structures and with each cell having a four-bar mechanism, the local deformation of one cell leads to the transformation of adjacent cells, resulting in the global transformation propagated throughout the metamaterial structure. Later in the design phase, the edge components were modified to have slots and notches for the insertion and mounting of electronic components of the sensor.

After the cell design was complete, measurements for the electronic components were taken followed by the 3D modeling of the individual building blocks. For this project, we created models in Autodesk Inventor Professional for cell flexures and edge components as seen in Figure 4.

After exporting the design files, the next step is the fabrication

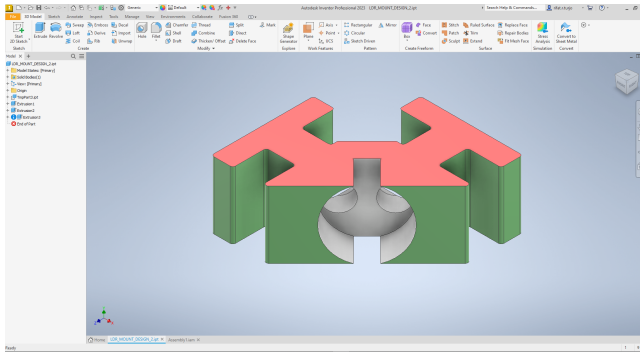


Figure 4: Design of edge component in Autodesk Inventor.
The notched section allows for the insertion of the LED.

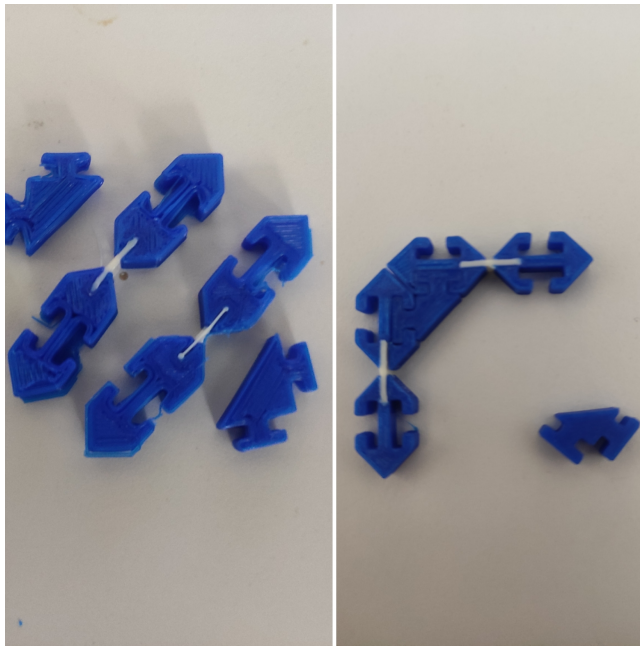


Figure 5: 3D printed components(left). Assembly of components(right).

of the components and the results can be seen in Figure 5. After connecting all of the parts we have our first metamaterial light sensor unit as seen in Figure 6.

2.2 Sensor Circuit Design

Figure 7 shows the complete prototype circuit used in the project. An Arduino Nano board was used to power the circuit and process raw data of the light-dependent resistors (which we refer to as the sensor 0,1 and 2) as analog inputs in real-time. A potentiometer was mounted to the sensor whose shaft undergoes rotation with the deformation of the sensor. The readings from the potentiometer are used as a reference for ground truth reading so as to compare

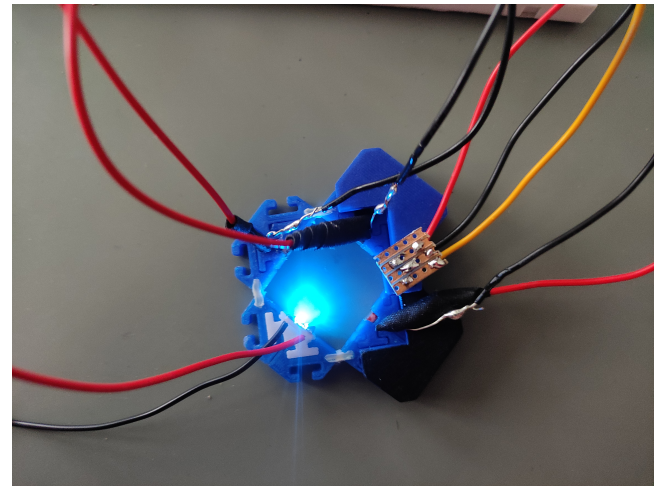


Figure 6: 3D printed metamaterial light sensor.

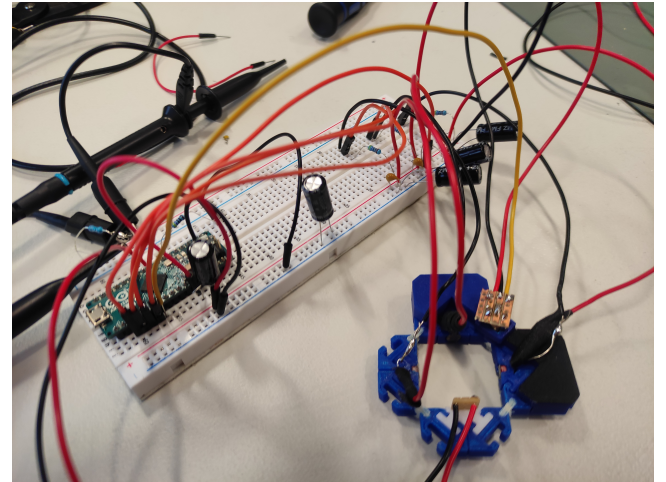


Figure 7: Metamaterial light sensor connected to the prototype circuit board.

and contrast with our sensor readings when cell deformation occurs. Electrolytic and ceramic capacitors are used to smooth the voltage on the power rails to reduce noise and cross-influence of the different sensors and the LED.

2.3 Sensing Principle

During the physical deformation of the sensor, the LED points more toward one particular light sensor than the other two. For measurements (in calibration and deployment) we pulse the LED and take a measurement with the LED on and one with the LED off and take the difference. This eliminates most of the influence caused by ambient light. Due to non-linearity in the LDRs and circuitry, some influence of the ambient light is left for that we compensate. After compensation, we use sensor fusion to get an

estimate of the deformation angle of one of the flexures. We aimed for and achieved a sampling frequency of at least 500 Hz.

2.4 Experimental Procedure

For calibration and evaluation, we did multiple tests with and without deformation at different ambient light levels. For calibration of the ambient light level compensation, we varied the ambient light level while not deforming the structure. One test was conducted in darkened conditions where the sensor was deformed to calibrate the sensor fusion using the readings from the potentiometer. Other tests were conducted in mid to high-light levels to evaluate the sensor.

2.5 Software Implementation

After having collected sensor data, we proceed with data analysis. Our overall goal is to calibrate the ambient light compensation for each sensor and then later implement a sensor fusion technique to correctly predict deformation parameters. Initially, for each sensor, we map the relationship between the raw values when the LED is off l_{off} , l_{1off} , l_{2off} to the difference delta in sensor value when the LED is pulsing $\Delta l = l_{on} - l_{off}$

The results for each sensor can be seen in Figure 8. It can be observed that without any compensation there appears to be a linear relationship between the two quantities. This allows us to easily compensate for the remaining systematic influence of ambient light by adding a compensation value that is linearly dependent on the l_{off} value to each data point, giving us our compensated values for Δl_0 , Δl_1 , Δl_2 . The gradient of this linear relationship is also stored to allow to use of the same compensation in deployment. From here on we will only refer to the compensated values.

The next step is sensor fusion. Our goal here is to use all three Δl values to efficiently estimate the potentiometer value. This can later be linearly mapped to the deformation angle of one of the flexures. We use a statistical approach to sensor fusion.

$$potest = argmax_x(p(x|\Delta l_0) * p(x|\Delta l_1) * p(x|\Delta l_2)) \quad (1)$$

With Bayes' Rule this is equivalent to

$$potest = argmax_x(\frac{p(\Delta l_0|x) * p(x)}{p(\Delta l_0)} * \frac{p(\Delta l_1|x) * p(x)}{p(\Delta l_1)} * \frac{p(\Delta l_2|x) * p(x)}{p(\Delta l_2)}) \quad (2)$$

Since we consider $p(x)$ constant over the whole deformation range and the $p(\delta l)$'s are not dependent on x this is equivalent to

$$potest = argmax_x(p(\Delta l_0|x) * p(\Delta l_1|x) * p(\Delta l_2|x)) \quad (3)$$

For our purpose, we can consider $p(\Delta l|x)$ and $p(x|\Delta l)$ equivalent. First, we fit a polynomial $\Delta lm(x)$ function to the Δl values of each sensor. Next, we calculate a smoothed deviation of the δl values around our fitted polynomials (visualized as red areas in fig. 10). Alongside that, we also fit a polynomial $\Delta lsd(x)$ to the deviation (seen in fig 11 and 12). When assuming that for a given deformation the Δl readings are normally distributed and the mean and standard

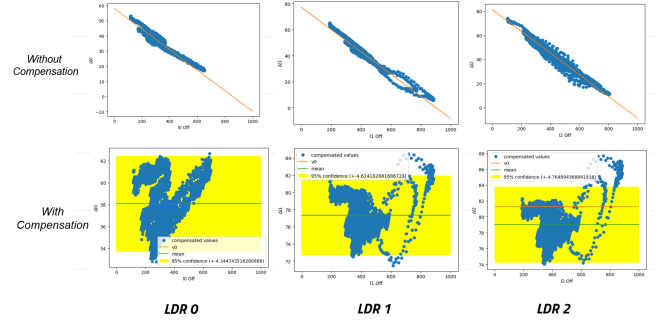


Figure 8: LDR sensor values for each sensor when the LED is off versus the difference delta of 1 between off and on. Top: Values without compensation. Bottom: Values with Compensation.

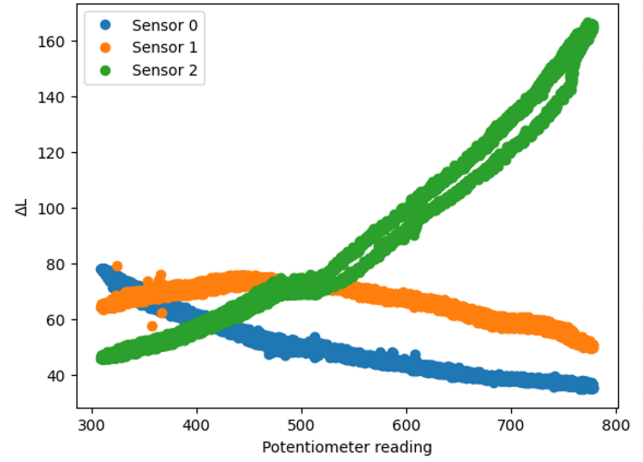


Figure 9: Deformation Calibration for each sensor.

deviation can be expressed by our polynomials we can calculate

$$p(\Delta l|x) = \frac{1}{\Delta lsd(x) * \sqrt{2\pi}} * exp(-\frac{1}{2} * (\frac{\Delta l - \Delta lm(x)}{\Delta lsd(x)})^2) \quad (4)$$

This gives us our first way to calculate $potest$. This is shown in fig 13 for the example values of $\Delta l_0 = 50, \Delta l_1 = 75, \Delta l_2 = 75$. Our remaining problem is that evaluating $argmax_x(p(\Delta l_0|x) * p(\Delta l_1|x) * p(\Delta l_2|x))$ is not that trivial to do analytically and evaluating it discretely is computation heavy to run real-time on a microprocessor. Additionally, the calibration lookup that would be needed to be stored would be quite large. Our solution is to evaluate $argmax_x(p(x|\Delta l_0) * p(x|\Delta l_1) * p(x|\Delta l_2))$ analytically. Therefore, we approximate $p(x|\Delta l)$ by a Gaussian bell function $g_{\Delta l}(x)$ (in the case of sensor 1 with two bells). They provide us with a very good fit and the maximum of their product can easily be evaluated analytically. (see fig 14 for fitted functions.) To fit the Gaussian functions we discretely evaluate $p(\Delta l_i|x)$ for changing x . This allows us to shrink our lookup to two values per possible Δl per sensor ($\sigma_{<sensor>}(\Delta l)$ and $\mu_{<sensor>}(\Delta l)$). And for evaluating $argmax_x(p(x|\Delta l_0) * p(x|\Delta l_1) * p(x|\Delta l_2))$ we can now analytically

reduce that to

$$pot_{est} = \frac{m}{\sigma_0(\Delta l_0) + \sigma_1(\Delta l_1)\sigma_2(\Delta l_2) + \sigma_2(\Delta l_2)\sigma_0(\Delta l_0)} \quad (5)$$

with

$$\begin{aligned} m = & \mu_0(\Delta l_0)\sigma_1(\Delta l_1)\sigma_2(\Delta l_2) + \mu_1(\Delta l_1)\sigma_0(\Delta l_0)\sigma_2(\Delta l_2) \\ & + \mu_2(\Delta l_2)\sigma_0(\Delta l_0)\sigma_1(\Delta l_1) \end{aligned} \quad (6)$$

This can now be easily calculated in real-time.

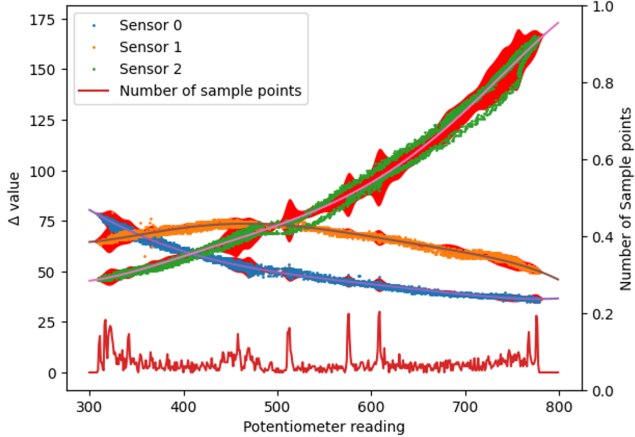


Figure 10: Plotting the uncertainty around the curve for each sensor.

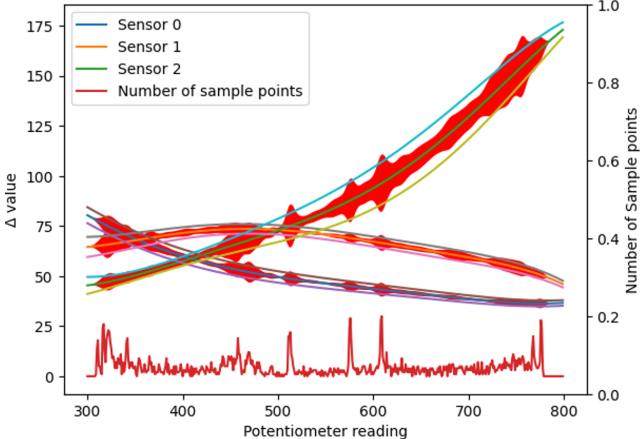


Figure 11: Approximating the uncertainty of the curves for each sensor.

2.6 Experimental Results

Lastly, the actual potentiometer reading upon deformation of the cell can be compared and contrasted with the estimated potentiometer readings obtained from the sensor fusion implementation, seen in Figure 15. To get accuracy for our sensor we then calculated the deviation between actual and predicted values. This gives us a 95% confidence interval of +/- 21.565 in terms of raw potentiometer readings which is equivalent to 7.76 degrees for the sensor deformation

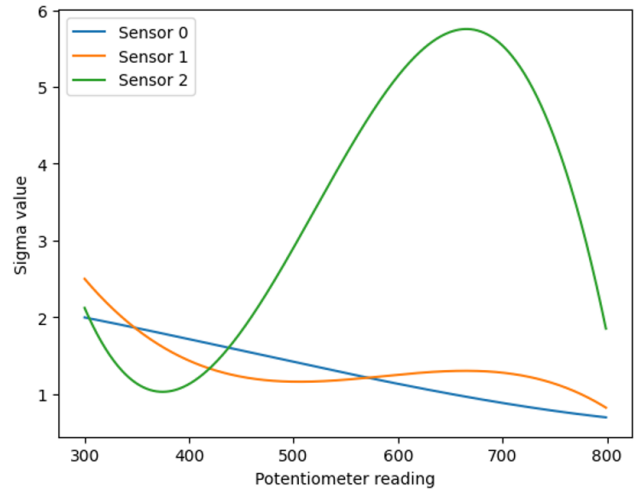


Figure 12: Deviation of sensor values over Potentiometer readings.

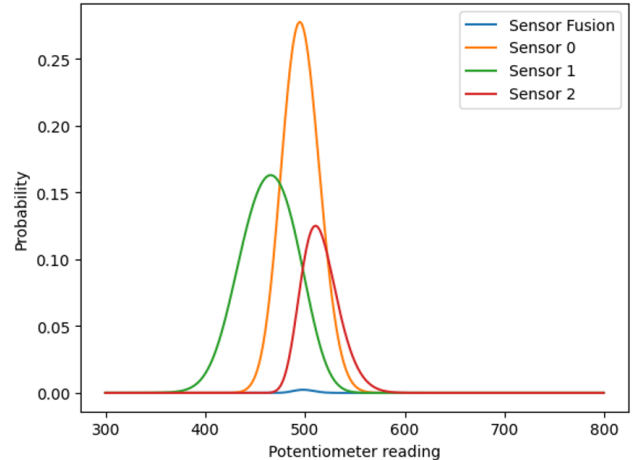


Figure 13: Potentiometer reading versus standard deviation for each sensor.

angle. The confidence interval is visualized in fig 15 by the orange lines. The data present between the standard deviation interval is our final estimated potentiometer reading using our LDR sensors. There is a noticeable noise in these readings but an FIR filter was sufficient in removing the noise for our real-time visualization.

2.7 Data Visualization

After having completed the sensor fusion, a Python script was written that visually represents the continuous deformation sensing of the metamaterial light sensor. In Figure 16, we see that the metamaterial light sensor is being deformed and in the application, the window demonstrates the deformation of a virtual metamaterial light sensor model in real-time. A 1st-order FIR filter was also implemented to eliminate high-frequency noise from the prior results.

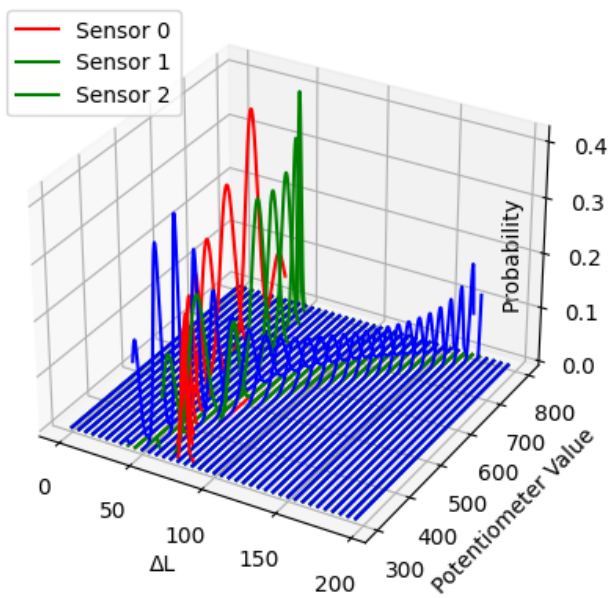


Figure 14: Gaussian curve distribution of the ΔL readings for each sensor versus their equivalent potentiometer readings.

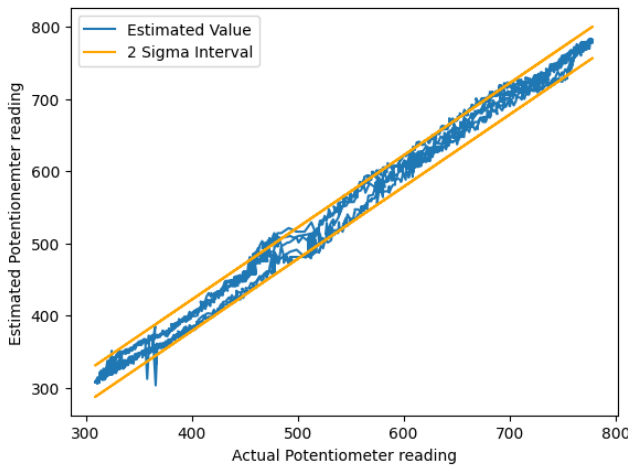


Figure 15: Sensor fusion implementation resulting in the mapping of actual potentiometer reading versus estimated potentiometer reading of sensors.

The sensor is able to approximate and visualize the real-time deformation of the metamaterial structure.

3 LIMITATIONS & FUTURE DIRECTIONS

Creating metamaterial sensors whose sensing capabilities are on the basis of light poses certain limitations. The largest limiting factor is the influence of ambient light. It produces a common signal far greater in comparison to the delta signal value that we are trying to

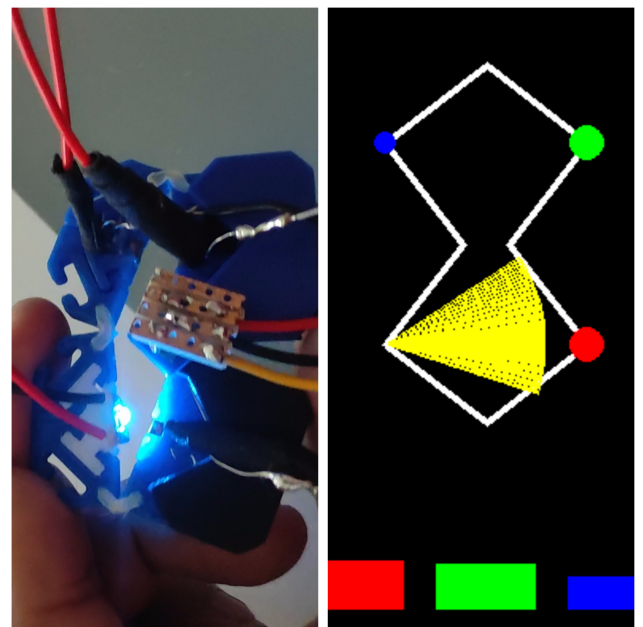
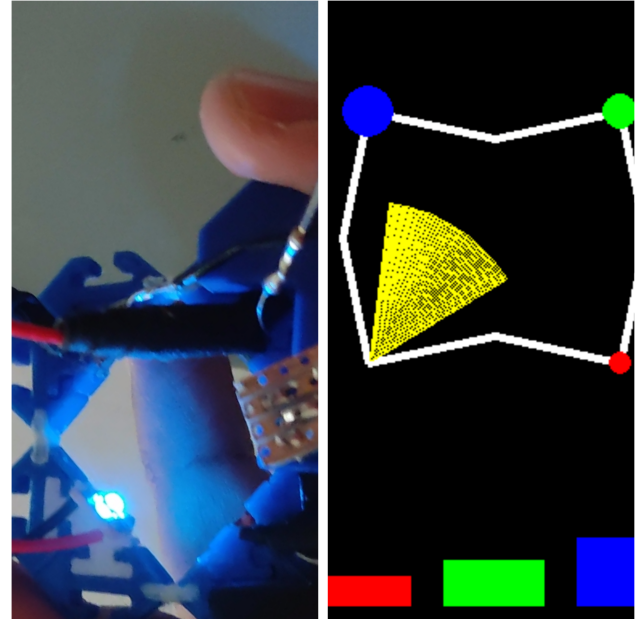


Figure 16: Cell deformation of physical metamaterial light sensor(left) and visualization in software (right).

measure for the light-dependent resistors. Although digital compensation was able to minimize its effect, rapidly changing light sources still pose a problem affecting the measured signals. Additionally, when held at certain angles, soft shadows from flexures and other components may be cast onto the light-dependent resistors which can influence the accuracy of the readings to a small degree. These problems however do not persist when the operations are carried out with the sensor in darkened conditions. Therefore, we aim to

review and refine signal-filtering and sensor fusion techniques to further mitigate the effects of external light sources.

Secondly, a potentiometer was used to obtain ground truth values to check the validity of our sensor readings. However, play in its mechanical construction had a noticeable negative effect on our calibration and evaluation. A more accurate ground truth reading would probably improve our accuracy substantially. In the future, we aim to modify the cell structure design to better incorporate surface-mounted components on flexible printed circuit boards. This will drastically reduce the number of electrical connections needed as well as minimize electrical interference. We also aim to substitute the potentiometer for a component able to provide more reliable and consistent ground truth readings.

4 CONCLUSION

In this project, a novel design for a metamaterial light sensor was proposed with the goal of being able to measure the continuous deformation of a metamaterial structure. An electronic circuit was embedded into the metamaterial device and the different sensor readings were measured as the structure underwent deformation. In the software implementation, a visualization of the physical deformation occurring in real time was achieved with the aid of signal filtering and sensor fusion techniques. In the future, we aim to improve and refine every aspect from 3D fabrication to circuit design to software implementation to better understand the feasibility of light-based sensing techniques for metamaterials.

5 ACKNOWLEDGEMENTS

The authors would like to thank Ata Otaran, Marie Muehlhaus and Prof. Dr. Jürgen Steimle, and all other members of the Human-Computer Interaction Lab at Saarland University for their guidance, assistance, and insight on the project throughout the Interactive Robotics seminar.

REFERENCES

- [1] Matthew J Chabalko, Jordan Besnoff, and David S Ricketts. 2015. Magnetic field enhancement in wireless power with metamaterials and magnetic resonant couplers. *IEEE Antennas and Wireless Propagation Letters* 15 (2015), 452–455.
- [2] Jing Chen, Wenfang Fan, Tao Zhang, Chaojun Tang, Xingyu Chen, Jingjing Wu, Danyang Li, and Ying Yu. 2017. Engineering the magnetic plasmon resonances of metamaterials for high-quality sensing. *Optics express* 25, 4 (2017), 3675–3681.
- [3] Charles El Helou, Philip R Buskohl, Christopher E Tabor, and Ryan L Harne. 2021. Digital logic gates in soft, conductive mechanical metamaterials. *Nature communications* 12, 1 (2021), 1633.
- [4] Alexandra Ion and Patrick Baudisch. 2019. Interactive metamaterials. *interactions* 27, 1 (2019), 88–91.
- [5] Alexandra Ion, Robert Kovacs, Oliver S Schneider, Pedro Lopes, and Patrick Baudisch. 2018. Metamaterial textures. In *Proceedings of the 2018 CHI Conference on Human Factors in Computing Systems*. 1–12.
- [6] Zachary H Nick, Christopher E Tabor, and Ryan L Harne. 2020. Liquid metal microchannels as digital sensors in mechanical metamaterials. *Extreme Mechanics Letters* 40 (2020), 100871.
- [7] Jifei Ou, Zhao Ma, Jannik Peters, Sen Dai, Nikolaos Vlavianos, and Hiroshi Ishii. 2018. KinetiX—designing auxetic-inspired deformable material structures. *Computers & Graphics* 75 (2018), 72–81.
- [8] Ke Wu, Xiaoguang Zhao, Thomas G Bifano, Stephan W Anderson, and Xin Zhang. 2022. Auxetics-Inspired Tunable Metamaterials for Magnetic Resonance Imaging. *Advanced Materials* 34, 6 (2022), 2109032.